

Automated Testbed for Repeatable Evaluation of Ultra-Wideband Localization Performance

Alexander Kemptner^{*†}, Julian Karoliny^{*}, Hannah Brunner[‡], Andreas Gaich^{*}, Michael Neubauer^{*}, Fjolla Ademaj-Berisha^{*}, Filippo Casamassima[‡], Walther Pachler[‡], Shrief Rizkalla^{*}, Harald Witschnig[‡], Andreas Springer[†], Hans-Peter Bernhard^{*†}

^{*}Silicon Austria Labs GmbH, Linz, Austria (alexander.kemptner@silicon-austria.com)

[†]Johannes Kepler University, Linz, Austria [‡]Infineon Technologies Austria AG, Graz, Austria

Abstract—Testing Ultra-Wideband (UWB) systems is challenging, as multiple devices need to coordinate over lossy links and the systems’ behavior is influenced by timing, synchronization, and environmental factors. Traditional testing is often insufficient to capture these complex interactions, highlighting the need for an overarching testbed infrastructure that can manage devices, control the environment, and make measurements and test scenarios repeatable. In this work, we present a highly automated testbed architecture built on Robot Operating System Version 2, integrating device management with environmental control and measurement systems. It includes an optical reference system, a controllable Autonomous Guided Vehicle to position devices within the environment, and time synchronization via Network Time Protocol (NTP). The testbed achieves a Root Mean Squared Error of 4.8 mm for positioning repeatability and 0.493° for the orientation, and our NTP-based synchronization approach achieves a timing accuracy of below 1 ms. All testbed functionality can be controlled remotely through simple Python scripts to allow automated orchestration tasks such as conducting complex measurement scenarios. We demonstrate this with a measurement campaign on UWB localization, showing how it enables repeatable, observable, and fully controlled wireless experiments.

I. INTRODUCTION

Evaluating the performance and firmware of wireless networks for applications like Ultra-Wideband (UWB) localization requires diverse functionality. For example, (i) devices need to be flashed with updated firmware, (ii) power and reset states need to be controllable to correctly initialize and start measurements, and (iii) logs must be collected to assess the localization performance afterwards. Additionally, not only do the devices need to be managed, but the environment should also be controllable and measurable. Therefore, a testbed’s functionality should also extend to infrastructure like Autonomous Guided Vehicles (AGVs) and optical reference systems. For UWB systems, this infrastructure is crucial to accurately measure localization performance. Unlike most testbeds, we use Robot Operating System Version 2 (ROS2) for our implementation. This significantly simplifies the testbed setup, as many infrastructure manufacturers provide pre-existing implementations for ROS2. Additionally, this allows for a centralized control of the whole testbed through a script or an interactive user interface.

In the literature, numerous testbeds for UWB performance measurements have been presented. One class of testbeds does not directly integrate the UWB devices into the testbed architecture, but instead uses a sniffer to record the data [1].

This enables a quick measurement setup for experiments with a focus on data post-processing. However, if many different chips or algorithms need to be tested, the manual orchestration of the devices (flashing firmware, starting/stopping measurements, etc.) becomes time-consuming.

More complex, fully integrated testbed setups for UWB are shown in [2], [3]. However, they also lack automation features like firmware updates on the devices, which are critical for quick evaluation of different algorithms. The testbed in [4] provides this automation in an integrated architecture using the Robot Operating System (ROS) (Version 1), but does not offer further functionality needed for UWB evaluation, like location ground truth measurements. The *Cloves* testbed presented in [5] also provides firmware flashing on a large scale, but no integration of AGVs or reference systems. Similarly, the testbed shown in [6] provides firmware flashing and log collection in a custom architecture, but assumes a fixed position of UWB devices, and does not provide live location ground truth measurements. The 5G testbed and measurement campaign reported in [7] includes UWB functionality, with the UWB subsystem implemented using an early version of the testbed presented in this paper. A fully integrated setup for UWB measurements based on ROS2 is used in [8]. However, the authors focus on measurement results and do not go into detail on the setup of the testbed itself. In summary, existing literature provides only limited descriptions of fully integrated UWB testbed architectures.

In this work, we want to fill this gap by providing a complete description of such a testbed capable of repeatable, automated UWB performance measurements. We do not solely focus on the Device-under-Test (DuT), but describe all components and their interconnections in detail. We build upon open source implementations which vastly accelerates implementation for readers interested in recreating our setup. In addition, we evaluate key performance aspects of the testbed itself, including its positioning and orientation repeatability as well as its time-synchronization capabilities for both wired and wireless orchestration. Finally, we demonstrate the system through a simple grid-based UWB localization example to showcase its end-to-end functionality.

The remainder of this work is organized as follows. In Section II, we introduce the general architecture of the testbed. In Section III, the hardware and software realization of this architecture is described in detail, which is the main contribution

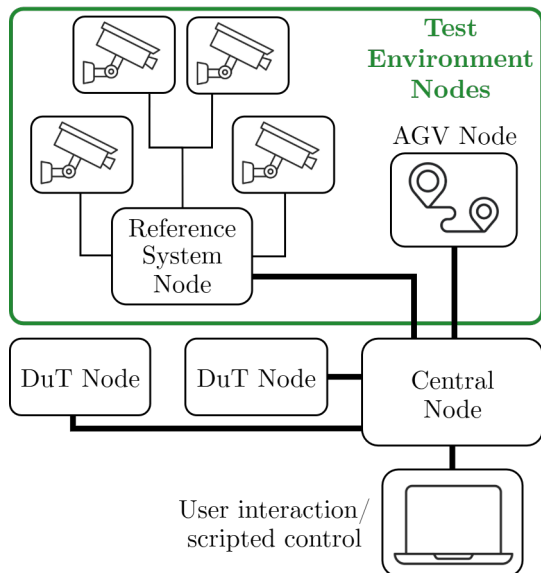


Fig. 1: Architectural overview of the testbed, its individual building blocks and their connections.

of this work. Section IV includes the performance evaluation of the testbed and shows results of UWB localization measurements using our setup.

II. TESTBED ARCHITECTURE

In this section, we highlight the architecture of our proposed testbed, the individual components, and how they are connected. The building blocks of the architecture are referred to as *nodes* in this work. An overview is outlined in Fig. 1, where the different node types are depicted. The types can be separated into the DuT nodes, a central coordination node, and test environment nodes. The test environment nodes control or interact with the environment, such as the reference system node or the AGV node. Together, the nodes form the architectural base of our fully automated wireless testbed.

A. DuT Nodes

The primary component of the testbed is the wireless device with the corresponding firmware that needs to be evaluated, which we refer to as Device-under-Test (DuT). In our proposed architecture, it is always paired with a Single-Board Computer (SBC) as a management device, which provides all testbed orchestration functionality. Together, they form a *DuT node*. The motivation for this is twofold. Firstly, the firmware of the DuT is not cluttered with testbed orchestration functionality like Over-the-Air (OTA) updates. Secondly, the wireless channel used by the DuTs is free from interference, as the management device can use a communication technology different from the DuT. In the case of our proposed UWB testing, the management can be performed via WiFi or Ethernet without interfering with the UWB communication. The separation in both firmware and communication channel ensures that measurements only evaluate the DuT performance, while not being influenced by orchestration tasks. The main functionalities of

the DuT nodes are turning the DuT on and off, interacting with the firmware, or gathering measurements or logs.

B. Test Environment Nodes

Although the DuTs are the main focus of the wireless communication testing, the interaction with the environment is also important. In wireless testing, precise and repeatable measurements are only achievable within a controllable and observable environment. Therefore, in addition to the DuT nodes, our testbed architecture incorporates *test environment nodes*. This category includes all devices capable of either manipulating or monitoring the environment. Examples of manipulations include altering the positions of environmental objects or adjusting conditions such as lighting and temperature. Conversely, environmental state measurements include activities such as object tracking or monitoring physical parameters. The green box in Fig. 1 highlights two examples of these node types which are used in our testbed. One of these nodes is the AGV node. Its purpose is to vary the location of objects in the environment for measurement purposes. As an example, a DuT node could be moved by the AGV to assess its behavior under varying spatial configurations. The architecture is flexible with respect to the specific type of AGV. This could be a ground-based robot, a drone, or another vehicle. The second node is a monitoring node to record the ground truth of locations. In our testbed, this reference system node manages a set of highly precise reference cameras.

C. Central Node and User Interaction

The core of the testbed is the central node, which connects all individual nodes as illustrated in Fig. 1. The testbed follows a star topology, with the central node serving as the primary communication hub. It is responsible for maintaining connections with the devices and coordinating various tasks, such as sending control commands to the other nodes and recording measurements. Another key function of the central node is to provide time synchronization services to all individual nodes, ensuring a common and consistent time base across the system. In addition to managing internal network communication, the central node also serves as the main user interface. Users can interact with the system either by sending commands to the central node interactively or through scripted workflows. The latter allows for automated and repeatable orchestration tasks such as conducting complex measurement scenarios. Importantly, the user interacts only with the central node. Commands directed to other nodes, e.g., to the DuT node, are always routed through the central node, which handles the coordination and dispatch of these tasks to the respective devices.

III. TESTBED REALIZATION

In this section, the realization of the aforementioned testbed architecture is described in detail. In particular, we will focus on the communication between the individual nodes shown in Fig. 1 and the protocols used to implement this communication. To ensure implementation efficiency and reproducibility, standard and openly available protocols and middleware frameworks were employed. Specifically, ROS2

was chosen for inter-node communication, Network Time Protocol (NTP) for time synchronization between nodes, and a Representational State Transfer (REST) Application Programming Interface (API) for user interaction with the central node. These technologies were selected not only for their technical suitability but also because they are open standards and widely supported. This choice provides a robust foundation for future extensions and facilitates the adoption and replication of the testbed by other researchers.

A. Orchestration with ROS2

The major part of the communication in the testbed occurs between nodes. For this purpose, ROS2 is used [9]. The support for multiple communication patterns, provided software tools, as well as pre-existing integrations from many manufacturers led to this choice. Originally, ROS2 is a software platform for building robot systems. It provides much of the functionality often needed in these systems and can be extended to fit the specific system with custom code written in C++ or Python. While robot systems are different from a wireless testbed, many of the challenges they face are similar. Both are composed of interconnected nodes, often running on different hosts, which need to work together to achieve a common goal. The interconnection of the nodes requires mechanisms for node discovery and communication, potentially across heterogeneous wired and wireless links as well as different operating systems. ROS2 provides all of these capabilities. Its widespread adoption is further reflected by the many device manufacturers that already provide code to integrate their products into ROS2 systems. This includes AGV and optical reference system manufacturers. Other protocols, such as MQTT, as used in the 5G testbed in [7], can achieve comparable orchestration. However, much of the functionality and synergies that ROS2 provides out of the box would have to be implemented manually.

1) *Networking and Data Exchange*: In terms of networking, ROS2 serves as a middleware and one of the key features provided is peer-to-peer discovery. This means that nodes do not need to know the IP addresses of other nodes to communicate with them. Rather, they can be addressed by name or enumerated by type (e.g. all DuT nodes). This is possible even without a central server. Therefore, the central node shown in Fig. 1 is not a requirement from ROS2, but a deliberate choice in our architecture to have a central orchestration hub. Messages can be exchanged in three different communication schemes. As illustrated in blue in Fig. 2 for the DuT node, these schemes are characterized as follows:

Topics follow a publish-subscribe pattern. This means that one or many nodes can publish to a specific topic. Nodes can subscribe to this topic and receive the messages.

Services provide a client-server pattern. The node acting as a client can send a request to a specific node, which answers with a response. The requester waits for the response, so the node is required to answer in a timely manner.

Actions are a mix of topics and services. A client node sends a request to the server node. The server node starts a long-

running task and signals the start via an initial response. Progress can be messaged back to the client node via a topic. When the task finishes, a response is sent.

For both discovery and communication, ROS2 builds upon Data Distribution Service (DDS), which is an open communication standard. It offers configurable Quality of Service (QoS) parameters, which can be used to adjust the communication to available bandwidth, allowed latency, or other requirements. For example, sensor values sent through a topic are not retransmitted if communication errors occur when the QoS setting *reliability* is set to *best-effort*. Similarly, the application is notified if no values are received for a specified time by setting the QoS setting *deadline* to this time [9], [10]. In addition to its flexibility, studies show good performance of the DDS protocol in terms of round-trip times [11].

2) *Example Link – Central to DuT Nodes*: The communication between a DuT node and the central node is shown in detail in Fig. 2. As explained in Section II-A, a DuT node consists of a management device and one or more DuTs. They are connected via serial over USB, which is indicated by the green arrows. The management device handles all further communication to the testbed. Communication shown with blue arrows is done via ROS2. All three communication schemes provided by ROS2 are used. The serial log is streamed to the central as a topic which supports multiple nodes subscribing and publishing to it. Services are used for commands controlling the DuT board. Finally, as flashing the complete firmware is a longer-running task, it is implemented as an action.

B. Time Synchronization Strategy

In automated testing, reliable measurements are essential, and their validity depends on precise timestamping of the measurements and other relevant events. Additionally, accurate synchronization enables faster measurement campaigns, as guard intervals between individual measurements can be kept shorter. To achieve the highest possible accuracy, timestamping is performed directly at the DuT node, i.e., at the moment when the UWB DuT sends the information to the SBC. The corresponding timing information is then forwarded to the central node via the ROS2 logging topic. Compared to timestamping at the central node, this approach avoids additional latency and jitter introduced by ROS2 communication, resulting in more precise timing data. Since ROS2 itself does not provide time synchronization [12], the host systems running the ROS2 nodes are synchronized using NTP. This is preferred over the more precise Precision Time Protocol (PTP), as the latter requires all nodes to be connected via Ethernet, and requires special hardware support [13], which is not feasible for mobile AGV and DuT nodes. After the synchronization procedure, ROS2 uses the clock of the host system for timestamping. In our architecture, the NTP server runs on the central node, while all other nodes operate as clients synchronizing to it. This is indicated in Fig. 2 by the yellow arrow. This setup provides sufficient accuracy for the testbed, even over WiFi, as evaluated in Section IV-B.

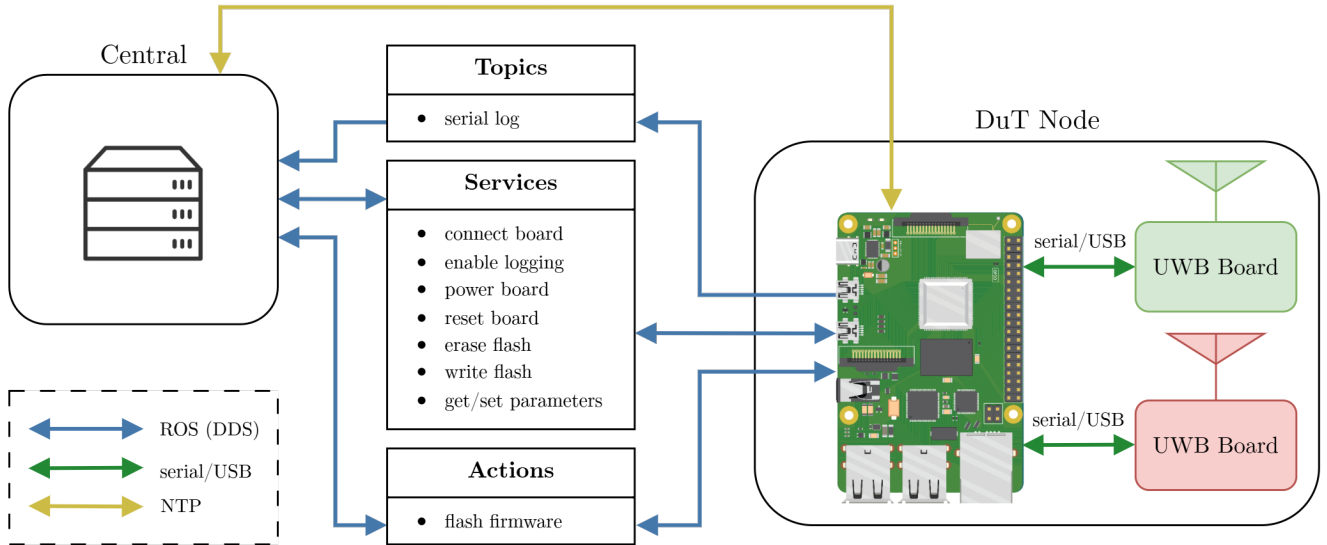


Fig. 2: Detailed block diagram of information and command flow between the central node and the UWB node.

C. User Interaction and Automation API

All internal communication between the central node and other nodes is handled using ROS2. The user interacts with the testbed exclusively through the central node. It processes the commands and forwards them as needed. Unlike the internal node communication, the interaction between the user and the central node is based on a REST API. This approach combines simple interaction with the testbed via REST, while maintaining time-critical orchestration via ROS2. This way, no ROS2 installation is required on the user's device. Additionally, the REST API offers a well-defined abstraction, which can be used for both interactive and scripted control of the testbed. More specifically, we provide a dedicated interactive web interface as well as a Python API as user interfaces.

As indicated in Fig. 2, the testbed provides extensive functionality to control the DuT nodes. Users are able to control power to the DuT devices, which works by switching the USB port on or off. If powered, users have the option to connect the serial port and enable logging. This starts sending logs via the logging topic. Parameters like serial port and baudrate are set and read using the parameter feature provided by ROS2. Users are able to control the firmware on the board by resetting it, erasing the flash memory, or by flashing a new firmware. The latter is implemented as an action, as it is a long-running task. After the user initiates flashing, the central node sends the firmware binary within the ROS2 request message, which the DuT node confirms with a response. After flashing is finished, the DuT node signals this to the central node with another response. As an alternative to writing the complete flash, writing to a specific flash address is also possible, allowing for device-specific configuration such as unique IDs to be set directly in the flash.

A similar level of control is available for the test environ-

ment nodes. For example, the AGV can be moved to a specific location and orientation and provides internal odometry sensor data, while the reference system node offers access and control of the ground truth location measurements.

D. Software and Hardware Setup

For the realization of the testbed, we aimed to utilize existing software components as much as possible to allow easy integration of our proposed architecture. This approach highlights one of the key advantages of ROS2, namely the extensive availability of open-source implementations. For these existing building blocks and nodes, we do not explicitly list the communication endpoints, but instead refer to the respective open-source projects. The reference system node is based on the MOCAP4ROS2 project [14]. The AGV node employs the ROS2 packages provided by the manufacturer, Husarion. For NTP-based time synchronization among the nodes, *chrony* is used on both the client side (DuT, reference system, and AGV nodes) and the server side (central node) [15].

The main components designed and implemented specifically for the presented testbed are the DuT and the central node. As shown in Fig. 2, the DuT node mainly reads and forwards logs from the serial interface and translates received control commands to OpenOCD commands. The central node primarily serves as a bridge between asynchronous user commands and their distribution within the ROS2 domain. As mentioned earlier, this bridging functionality is realized through a REST API, implemented using the FastAPI framework. The interactive web interface for system control is hosted by the central node and served via the open-source nginx web server.

While the proposed architecture is designed to be flexible with respect to the underlying hardware, the following setup was selected for our realization. The managing part of each

DuT node is realized using Raspberry Pi 5 SBCs, while the DuT itself combines a PSoC6 CYBLE-416045 evaluation board with a Quorvo DWM3000EVB UWB module. The reference system consists of twelve Prime^x 22 cameras by OptiTrack with an accuracy of ± 0.15 mm. For the AGV, the ROSbot XL by Husarion is used. The reference system node and central node are hosted on laptops running Ubuntu 24.04. The software setup on all components is containerized using Docker, including all ROS2 installations as well as the chrony and nginx services. This approach ensures a reproducible and consistent software environment across all devices.

IV. EVALUATION: UWB CASE STUDY

In this section, we evaluate the presented functionality of the testbed, including an indoor grid-based UWB localization as an example application. All measurements are carried out through the Python scripting interface of the testbed. The UWB setup consists of $N = 4$ anchors with a fixed and known position on the ceiling in a typical lab environment, and one tag, which is placed on the AGV. The firmware and configuration for these individual roles are directly flashed onto the corresponding DuT nodes at the beginning of the measurement scripts by the automated testbed. All DuT nodes operate on UWB channel 9 (7987.2 MHz) at a bandwidth of 499.2 MHz.

In the first evaluation, we investigate the positioning repeatability achievable through the combination of the AGV and the optical reference system. Then, we evaluate the synchronization accuracy achievable between DuT nodes with the described NTP solution. Lastly, we demonstrate the testbed end-to-end by executing a simple localization measurement campaign.

A. Positioning Repeatability

To evaluate the positioning repeatability, a fixed reference position and orientation in the room was selected. The AGV was sent to this position and orientation, followed by a random position and orientation within a grid of 2x2m, then back to the reference position again. This alternating pattern was repeated 100 times. For each position, the real position was measured using the optical reference system and compared to the target. The central node employs a PID controller for moving the AGV to the defined position within a configurable threshold. Although the controller also uses the very precise reference system as position input, typically there are still differences between the target and real positions due to mechanical constraints of the AGV and the chosen maximum allowed speed. The thresholds were set to ± 0.5 cm/ $\pm 0.3^\circ$ and the maximum speed to 0.1 m/s. This resulted in a Root Mean Squared Error (RMSE) for the positioning of approximately 4.8 mm. An additional error measure is the Circular Error Probable 95 (CEP95), which describes the radius that includes 95% of measurements. In our measurements, the CEP95 is approximately 9.32 mm. This proves that overall, the system is capable of repeatable centimeter-level positioning. Similarly, the orientation RMSE was approximately 0.493° , which is especially important when evaluating DuTs with directional antennas.

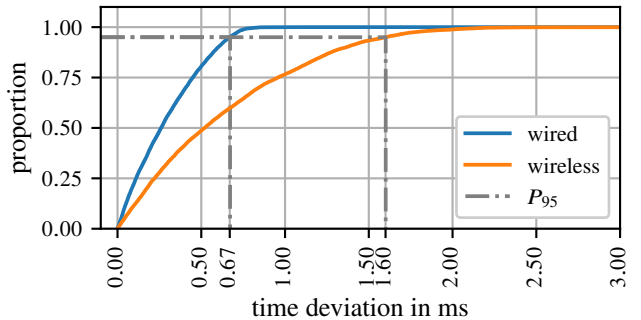


Fig. 3: CDF of NTP synchronization accuracy over wired vs. wireless link.

B. Synchronization Accuracy

To evaluate the NTP synchronization accuracy, four DuT nodes were connected to the central node over a 5 GHz IEEE 802.11ac wireless link. The DuT node used as the tag was disregarded for this measurement. The NTP was configured to dynamically synchronize every 16 to 256 s. To generate log output, a firmware was flashed onto the DuT, which writes to the serial interface upon registering a rising edge on a General Purpose Input/Output (GPIO) pin. As in normal operation of the testbed, this log is collected and timestamped by the SBC of the DuT node. For the measurement, the DuT nodes could synchronize for 30 minutes. Afterwards, the GPIO pins were triggered simultaneously at a frequency of 1 Hz for 30 minutes by an arbitrary waveform generator. Ideally, the four timestamps generated on each rising edge by the DuT nodes should be identical. However, imperfections in the NTP synchronization, as well as timing differences in the serial data transmission lead to deviations. These deviations are evaluated by comparing the timestamps for all combinations of two nodes for each rising edge. The results are shown as a Cumulative Distribution Function (CDF) in Fig. 3. For the wireless connection (orange line), 95% of nodes deviate by 1.6 ms or less. The RMSE of time deviations was approximately 0.81 ms. As mentioned in Section III-B, most test scenarios require at least some nodes to be connected wirelessly for mobility. However, fixed nodes in the testbed are typically connected over Ethernet. The performance for the wired scenario is shown by the blue line in Fig. 3. For 95% of nodes, the time deviation is reduced to 0.67 ms or less, and the RMSE was 0.36 ms.

C. Testbed-Driven Localization Results

To demonstrate the functionality of the testbed end-to-end, a simple measurement campaign was carried out. The DuT node on the AGV serving as the tag was moved to positions arranged in a 5x5 0.25 m grid pattern. In total, five of these grids were measured at different spots throughout the room in an area of 6 x 6 m. A zoomed view of one grid is shown in Fig. 4. The true positions measured by the optical reference system and captured by the reference system node are shown by the blue dots. Every time the target position was reached, a

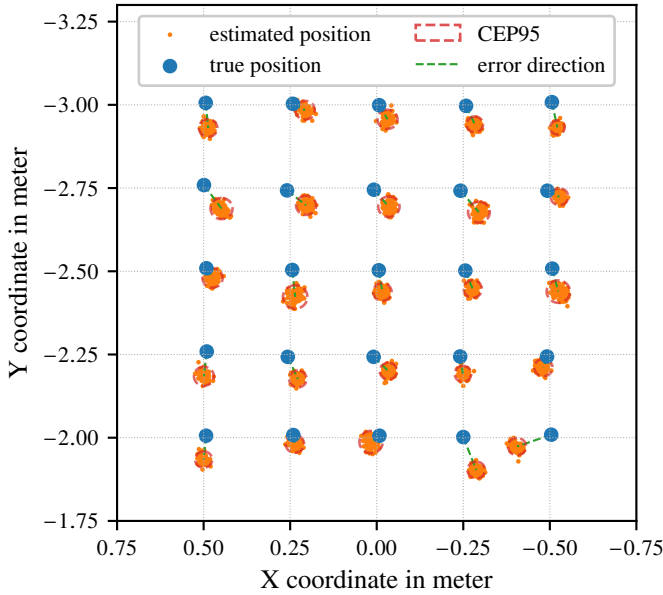


Fig. 4: View of a measured subgrid.

reset command was sent to the tag, which initiates 100 Double-Sided Two-Way Ranging (DS-TWR) [16] exchanges with each of the $N = 4$ anchors. This data was collected using the logging functionality of the testbed. Based on these distance measurements d_i , we estimate the position $\hat{\mathbf{p}} \in \mathbb{R}^3$ of the tag by solving the nonlinear least-squares problem

$$\hat{\mathbf{p}} = \arg \min_{\mathbf{p} \in \mathbb{R}^3} \sum_{i=1}^N (\|\mathbf{a}_i - \mathbf{p}\|_2 - d_i)^2, \quad (1)$$

where \mathbf{a}_i denotes the position of the i -th anchor. We solved this using the Levenberg-Marquardt algorithm. This leads to 100 estimated positions per true position, which are shown as orange dots. The RMSE of the position accuracy across all grids is 14.56 cm. The red circles show the CEP95 for each position, which visualizes the precision of the position estimation. On average, the radius of these circles is 5.09 cm. The green lines link the true position to the median of the estimated positions. The length of this line visualizes the accuracy of the position estimation. The mean length of these lines is 9.39 cm.

V. CONCLUSION AND FUTURE DIRECTIONS

This work presented a testbed architecture for UWB performance measurements. The testbed adopts a flexible architecture covering all aspects needed, like control of DuTs, reference systems, and AGVs. The flexible architecture allows for deployments at new sites with minimal reconfiguration. For internal communication, a hybrid approach was adopted, which uses ROS2 for time-critical internal communication, and a REST API for the user interface. Both communication protocols have extensive open-source and manufacturer support, which cuts down implementation efforts. As ROS2 does not provide synchronization between nodes, an NTP

implementation was deployed and tested, which leads to good synchronization errors of below 1.6 ms for 95% of nodes, also over wireless links. The testbed was evaluated with a simple localization measurement, which demonstrates its end-to-end functionality. Using DS-TWR exchanges, a RMSE of 14.56 cm was achieved compared to the ground truth provided by the integrated optical reference system. Most importantly, the testbed is capable of automated measurements with high repeatability. By simply executing a Python measurement script again, performance comparisons with updated firmware or different UWB chips can be executed quickly. With these features, our testbed will support the development, testing, and ultimately the adoption of many future UWB applications like the FiRa Hero Use Cases [17] of untracked navigation, public transport fare collection, and asset tracking.

REFERENCES

- [1] P. Peterseil, B. Etlzinger, R. Khanzadeh, and A. Springer, "Trustworthiness Score for UWB Indoor Localization," in *GLOBECOM*, 2023.
- [2] U. Raza, A. Khan, R. Kou, T. Farnham, T. Premalal, A. Stanoev, and W. Thompson, "Dataset: Indoor Localization with Narrow-band, Ultra-Wideband, and Motion Capture Systems," in *Proc. 2nd Workshop on Data Acquisition To Analysis*. ACM, 2019, p. 34–36.
- [3] M. Delamare, F. Duval, and R. Boutheau, "A new dataset of people flow in an industrial site with UWB and motion capture systems," *Sensors*, vol. 20, no. 16, p. 4511, 2020.
- [4] L. B. Hörmann, A. Pötsch, C. Kastl, P. Priller, and A. Springer, "A Distributed Testbed for Wireless Embedded Devices," in *IEEE Int. Mediterranean Conf. Commun. Netw. (MeditCom)*, 2023, pp. 381–386.
- [5] D. Molteni, G. P. Picco, M. Trobinger, and D. Vecchia, "Cloves: A Large-Scale Ultra-Wideband Testbed," in *Proc. 20th ACM Conf. on Embedded Networked Sensor Systems*. ACM, 2023, p. 808–809.
- [6] M. Schuh, H. Brunner, M. Stocker, M. Schuß, C. A. Boano, and K. Römer, "First Steps in Benchmarking the Performance of Heterogeneous Ultra-Wideband Platforms," in *2022 Workshop on Benchmarking Cyber-Physical Systems and Internet of Things (CPS-IoTBench)*, 2022.
- [7] D. Hamidovic, A. Hadziaganovic, J. Karoliny, A. Gaich, D. Klepatsch, M. Ahmed, R. Muzaffar, A. Springer, and H.-P. Bernhard, "5G and UWB Integration for Robot Collaboration," in *IEEE IECON*, 2025.
- [8] P. T. Morón, S. Salimpour, L. Fu, X. Yu, J. P. Queraltá, and T. Westerlund, "Benchmarking UWB-Based Infrastructure-Free Positioning and Multi-Robot Relative Localization: Dataset and Characterization," in *2023 IEEE Sensors Applications Symposium (SAS)*, 2023, pp. 1–6.
- [9] S. Macenski, T. Foote, B. Gerkey, C. Lalancette, and W. Woodall, "Robot Operating System 2: Design, architecture, and uses in the wild," *Science Robotics*, vol. 7, no. 66, p. eabm6074, 2022. [Online]. Available: <https://www.science.org/doi/abs/10.1126/scirobotics.abm6074>
- [10] Open Robotics. (2025) Quality of Service Settings. Accessed Oct. 06, 2025. [Online]. Available: <https://docs.ros.org/en/jazzy/Concepts/Intermediate/About-Quality-of-Service-Settings.html>
- [11] S. Profanter, A. Tekat, K. Dorofeev, M. Rickert, and A. Knoll, "OPC UA versus ROS, DDS, and MQTT: Performance Evaluation of Industry 4.0 Protocols," in *2019 IEEE Int. Conf. on Ind. Technol. (ICIT)*.
- [12] Tully Foote. (2021) Time synchronization approaches. Accessed Oct. 07, 2025. [Online]. Available: <https://robotics.stackexchange.com/questions/99207/time-synchronization-approaches>
- [13] P. Kulthumrongkul, S. Hengyotmark, and W. Pora, "Implementation and Performance Analysis of PTP and NTP Servers on the Raspberry Pi CM5," in *2025 ECTI-CON*, 2025, pp. 1–5.
- [14] ROSIN. (2025) MOCAP4ROS2-Project. Accessed Sep. 30, 2025. [Online]. Available: <https://github.com/MOCAP4ROS2-Project>
- [15] M. Lichvar and R. Curnow. (2025) chrony. Accessed Oct. 07, 2025. [Online]. Available: <https://chrony-project.org>
- [16] D. Neirynek, E. Luk, and M. McLaughlin, "An alternative double-sided two-way ranging method," in *2016 13th Workshop on Positioning, Navigation and Communications (WPNC)*, 2016, pp. 1–4.
- [17] FiRa Consortium. (2025) Fira Annual Report 2025. Accessed Mar. 03, 2026. [Online]. Available: firaconsortium.org/sites/default/files/2026-02/FiRa_Annual_Report_2025.pdf